Electrosprayed Polymer Particles: Effect of the Solvent Properties

Chul Ho Park, Jonghwi Lee

Department of Chemical Engineering and Materials Science, Chung-Ang University, 221, Heukseok-Dong, Dongjak-Gu, Seoul 156-756, South Korea

Received 22 December 2008; accepted 15 March 2009
DOI 10.1002/app.30498
Published online 8 June 2009 in Wiley InterScience (www.interscience.wiley.com).

ABSTRACT: Electrospraying technology has been studied in many fields to produce particles of various substances from nanoscale to microscale sizes. Unlike pure liquids, droplets formed by electrospraying that are comprised of polymer solutions undergo additional solidification processes involving solvent evaporation, which primarily determine the particle size and morphology. Herein, the effects of the solvent properties on the morphology and dimensions of solidified particles were systematically studied. In general, the size of the solidified spherical particles with smooth surfaces reflected that of the initially formed liquid droplets, which could partially be estimated by theoretical equations developed for pure liquids. Particle sizes increased with an increase in polymer content and a decrease in the boiling point of the volatile solvent. Inhomogeneous drying processes related to phase separation or skin formation resulted in hollow, cuplike, and porous particle structures, with particle sizes and morphologies that were outside of the scope of the theoretical treatments. The selection of a proper solvent or solvent mixture seemed to be a convenient way to control the particle morphologies, such as hollow, cuplike, or porous structures. © 2009 Wiley Periodicals, Inc. J Appl Polym Sci 114: 430–437, 2009

Key words: fibers; macroporous polymers; nanotechnology; particle size distribution; polystyrene

INTRODUCTION

Polymeric nanoscale and microscale particles that are widely used in various applications, such as photonics,[1] electronics,[2] and drug delivery,[3] have been produced with several common technologies. Among them, emulsion and suspension polymerization[4,5] have advantages for controlling size distribution but have several drawbacks, such as inhomogeneous particle fabrication and a restricted number of processable polymers. Precipitation,[6] spray drying,[7] and supercritical fluid[8] processes can effectively produce polymeric particles; however, they can hardly generate monodisperse particles. Shirasu Porous Glass membrane emulsification[9] and solvent-evaporation technology[10] are useful methods for producing narrow size distributions. However, Shirasu Porous Glass barely generates nanoparticles smaller than 500 nm. The solvent-evaporation method requires a low polymer concentration (usually <0.05 wt %) to prepare nanoparticles.

Correspondence to: J. Lee (jong@cau.ac.kr).
Contract grant sponsor: Fundamental R&D Program for Core Technology of Materials funded by the Ministry of Commerce, Industry and Energy, Republic of Korea.

Journal of Applied Polymer Science, Vol. 114, 430–437 (2009)

Recently, electrospraying (electrohydrodynamic spraying) has been recognized as an alternative technology for overcoming the aforementioned limitations and generating interesting morphologies.[11,12] Four centuries ago, Gilbert[13] observed that electrical fields could deform fluid interfaces. Zeleny[14] showed that a sufficiently strong electrical field could destabilize an interface separating a drop from the surrounding air. The stability of charged droplets was theoretically analyzed by Rayleigh.[15] He predicted that an incompressible charged liquid droplet would become unstable as soon as the disruptive Coulomb force was equal to the attractive cohesive force, or, in terms of energies, when the Coulomb energy (CE) corresponded to twice the surface energy (SE). The Rayleigh limit (X) is defined as

$$X = \mathrm{CE}/2\mathrm{SE} = q^2/(64\pi^2\varepsilon\gamma R^3)$$

where q is the surface charge of a droplet, ε is the permittivity of the medium surrounding the droplet, γ is the surface tension of the liquid, and R is the radius of a droplet. Rayleigh suggested that the breakup of a droplet occurs when $X \geq 1$. Several modern experiments[16–18] have probed Rayleigh's original ideas on the stability of macroscopic liquid droplets, and the breakup of droplets was found for most cases below the Rayleigh limit. However, the Rayleigh limit parameters are still insightful for

understanding the breakup of highly charged droplets of various liquids.

In electrohydrodynamic spraying, an unstable and charged interface takes on a conical shape, referred to as a *Taylor cone*,[19] and a fine jet emitted from the cone's tip disintegrates into highly charged droplets, with magnitudes close to the Rayleigh limit.[20] Such electrohydrodynamic streaming and cone-jetting phenomena have been applied in various fields, such as the popular technique of electrospray mass spectrometry for assaying large biomolecules and the techniques of encapsulation, fine powder production, or thin-film deposition.[21–24]

The first step in electrospraying is droplet generation, which depends on the solution properties and processing parameters. Empirical equations have been developed for predicting the droplet sizes (dd) of neat liquids.[25,26] In the case of highly conducting liquids, a theoretical step forward has been made by Fernandez and Loscertales,[27] who found a scaling law for the spray current emitted from an electrified meniscus. Ganan-Calvo[28] formulated the following theoretical equation on the basis of a steady quasi-one-dimensional model having no mass loss, for which the scaling laws agreed reasonably well with experimental results:

$$d_d = \alpha\left(\frac{Q^3\varepsilon\rho}{\pi^4\sigma\gamma}\right)^{1/6} \quad (1)$$

where α is a constant depending on liquid permittivity, Q is the liquid flow rate, ε is the dielectric constant in a vacuum, ρ is the density of the liquid, σ is the surface tension of the liquid, and γ is the conductivity of the liquid. Ganan-Calvo demonstrated that electrospraying technology could fabricate monodisperse droplets.

A polymer solution having sufficient chain entanglement density (typically, $c/c^* > 3$, where c is the concentration of the polymer and c^* is the critical overlap concentration) will be electrospun instead of electrosprayed.[29] At a nonfiber-forming concentration (low chain entanglement density), the jet of a polymer solution disintegrates into fine droplets. The size of the droplets might be based on Ganan-Calvo parameters, but the same estimation is not readily applicable to the size of solidified polymer particles. Unlike pure liquids, the droplets of a polymer solution undergo additional particle-formation steps, such as consolidation and agglomeration. Consolidation mechanisms can be partially estimated by the Cahn-Hilliard equation.[30] However, it is still the case that the estimation of particle size and morphology in electrospraying cannot be satisfactorily achieved by theoretical equations because of complicated thermodynamic and kinetic parameters involved in the process.

Experimentally, several research groups have used electrospraying technology to produce polymeric particles for drug-delivery applications, whereas the relationship between processing parameters and particle properties has not been clearly studied.[31–33] Fantini et al.[12] studied polystyrene (PS) particles produced by electrospraying[12] and suggested that the morphology of solidified particles depends on the molecular weight of the polymer. Liu and Kumar et al.[34] demonstrated that the morphology of solidified poly (methyl methacrylate) was sensitively dependent on the type of solvent used.[34] They explained that the cuplike morphology of poly(methyl methacrylate) was produced because of solubility parameter differences.

The theoretical development of electrohydrodynamic jetting has claimed several advantages: (1) submicrometer particle size, (2) narrow particle size distribution, (3) absence of agglomeration and coagulation, (4) convenient encapsulation, and (5) high yield. Therefore, drug encapsulation by electrospraying seems to be attractive for the effective controlled release and improvement of drug stability required for drug-delivery applications. However, the approaches for drug encapsulation with a proper polymeric material have had problems because of the complex consolidation processes.[35–38]

Although there have been significant recent advances in the understanding of polymer electrospinning, the electrospraying of polymers has received relatively less attention with basic understandings of the technique left largely unexplored. Previous approaches for electrospraying liquid droplets have not provided sufficient understanding for the electrospraying of polymer solutions.[12,31–34] As mentioned previously, the morphology and size of polymer particles produced by electrospraying are complex functions of thermodynamic and kinetic effects. Herein, to understand the mechanisms involved in the consolidation of charged polymer droplets, the correlations between the morphology/size and processing parameters, that is, the solution properties (evaporation rates of solvents and concentrations) and other variables (flow rate, voltage, and ground-to-nozzle distance), were systematically studied. In particular, the solvent properties were closely monitored and found to be major factors in determining the morphology and size of solidified particles.

EXPERIMENTAL

Materials

PS (weight-average molecular weight = 45,000 g/mol) was purchased from Sigma-Aldrich (USA). The solvents (reagent grade) used in this study were

TABLE I
Physical Properties of the Solvents

Solvent	Conductivity (μS/cm)[a]	Surface tension (mN/m)[a]	Boiling point (°C)	R_{ij}[b]
MC	0.04	28	40	12.01
THF	0.04	26.3	66	9.73
Py	0.24	32.8	116	5.72
CC	0.04	35.2	142	8.13
DMF	1.2	36.5	146	13.13
An	0.04	29.2	147	7.62
BA	0.8	63.2	178	4.24

[a] Measured.
[b] $R_{ij} = [4(\delta_{1d} - \delta_{2d})^2 + (\delta_{1p} - \delta_{2p})^2 + (\delta_{1h} - \delta_{2h})^2]^{1/2}$ where δ is the Hensen solubility parameter; 1 and 2 denote the polymer and solvent, respectively; *d*, *p*, and *h* are the dispersion, polar, and hydrogen-bonding terms, respectively; and δ_{1d}, δ_{1p}, and δ_{1h} of PS are 21.3, 5.8, and 4.3, respectively.[50]

N,*N*-dimethylformamide (DMF), tetrahydrofuran (THF), methylene chloride (MC), pyridine (Py), cyclohexyl chloride (CC), anisole (An), and benzaldehyde (BA) and were purchased from Sigma-Aldrich. The physical properties of these solvents are presented in Table I. All chemicals were used without further purification.

Electrospraying

Figure 1 shows a schematic diagram of the electrospraying process (25°C, ~ 45% relative humidity). High-voltage direct current ranging from 0 to 30 kV was applied with a Convertech SHV model power supply (Seoul, South Korea). PS solutions were placed in a 5-mL polypropylene syringe (Henke Sass Wolf, Tuttlingen, Germany) with a 19-gauge stainless steel nozzle (i.d. = 0.69 mm, o.d. = 1.07 mm) and continuously pumped with a KD Scientific KDS100 syringe pump (Holliston, MA) with a control step rate of 10 μL/h. The ground-to-nozzle distance (or working distance) represents the distance from the tip of a nozzle to the ground. Electrospraying was performed for 5 min, and the electrosprayed particles were collected on a piece of aluminum foil (30 × 30 cm^2). After electrospraying, all of the samples were kept in plastic Petri dishes (diameter = 90 mm) for 1 day.

Characterizations

The conductivity of the polymer solutions (50 mL placed in vials) was measured with a Meterlab CDM210 conductivity meter (Lyon, France, conductivity accuracy = ±0.2%, two-pole CDC641T electrode). The surface tension was measured with the pendant drop method (stainless steel needle: i.d. = 0.2 mm, o.d. = 0.41 mm, ~ 40% relative humidity) with a Kruss DSA100 tensiometer (Hamburg, Germany, 50 fp/s). The surface tension values were automatically calculated from the fitting of the droplet shape (in a captured video image) into the Young–Laplace equation, which related interfacial tension to the droplet shape. Viscosity was measured with 30 mL of polymer solution in 50-mL glass vials and a Brookfield DV-II Pro viscometer with a cylindrical spindle (No. 1) (Middeboro, MA) at 6 rpm for 5 min. All values were obtained by the averaging of three measurements performed at 25 ± 5°C.

Scanning electron microscopy (SEM) images of particles were obtained with a Hitachi S-4800 (Tokyo, Japan) at 4 kV. Particles collected on aluminum foil were sputter-coated with platinum (thickness = 3 nm) with a high- resolution ion beam coater (model 682, Gatan, Pleasanton, CA). Scion image software (NIH, Bethesda, MD) was used to determine the average particle size by the calculation of the mean area of 100 particles.

RESULTS

Critical voltage for the polymer solutions

The application of voltage (*V*) generates electric potential (*E*) at a working distance (*H*) between a ground and a nozzle: $E = V/H$ (Fig. 1). When the interface between a conducting liquid and air is electrically charged beyond a critical level, the meniscus of the nozzle evolves from a rounded shape to a conical shape.

The conductivity and surface tension of PS solutions were almost independent of concentration (~ 0 to 7 wt % PS in DMF and THF, data not given). The surface tension and the conductivity of a miscible mixture of THF/DMF were found to follow a linear function: $P_{mixing} = v_1P_1 + v_2P_2$, where *v* is a volume fraction and *P* represents a physical property such

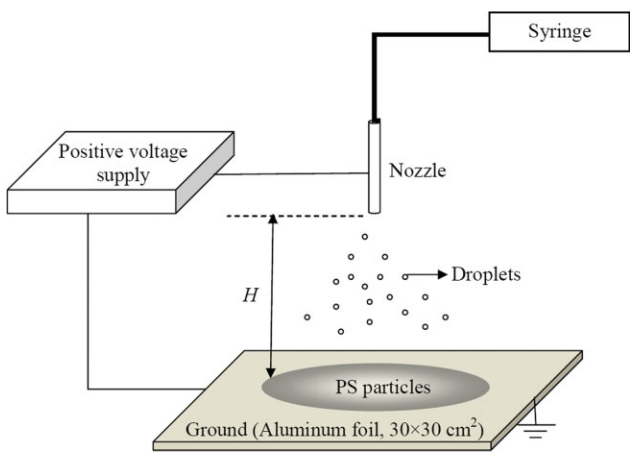

Figure 1 Schematic diagram of the electrospraying apparatus. *H* is the ground-to-nozzle distance.

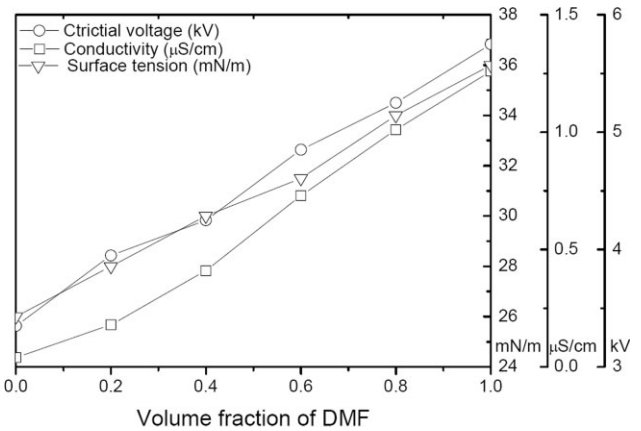

Figure 2 Critical voltage, conductivity, and surface tension as functions of the DMF volume fraction in a PS solution (THF/DMF mixed solvent). The electrospraying conditions were a ground-to-nozzle distance of 15 cm and a flow rate of 0.4 mL/h.

as surface tension or conductivity, as shown in Figure 2. When the volume fraction of DMF increased, the surface tension and conductivity increased, and the critical voltage for electrospraying also increased. This dependence was qualitatively consistent with Rayleigh's prediction.

For pure liquids, the critical voltage and the shape of the Taylor cone depend on the volumetric flow rate.[27,39,40] Figure 3 shows that the critical voltage for electrospraying was linearly proportional to flow rate. Below the critical voltage, the meniscus at the nozzle tip was dropped [Fig. 3(a)]. At a critical voltage defined for each flow rate, the meniscus at the nozzle tip elongated to the ground, which resulted in Taylor cone formation [Fig. 3(b)]. At voltages above the critical voltage, the jet tilted [Fig. 3(c)]. Beyond the critical voltage for multijets, several jet streams at the tip of the nozzle were observed [Fig. 3(d)]. This phenomenon was observed regardless of the flow rates used (valid within the range of flow rates examined). Therefore, the critical voltages for electrospraying polymer solutions followed qualitatively consistent dependencies on the flow rate and solution conductivity.

Morphology and size of the solidified particles

The ground-to-nozzle (working) distance determines the time of solvent evaporation when a droplet flies to the ground. Increasing the working distance decreases the applied electric potential but increases the travel time/distance of droplets, which relates to solvent evaporation. If a travel time is insufficient, droplets coat the ground plate as a film (droplet aggregation). To prevent apparent film formation on

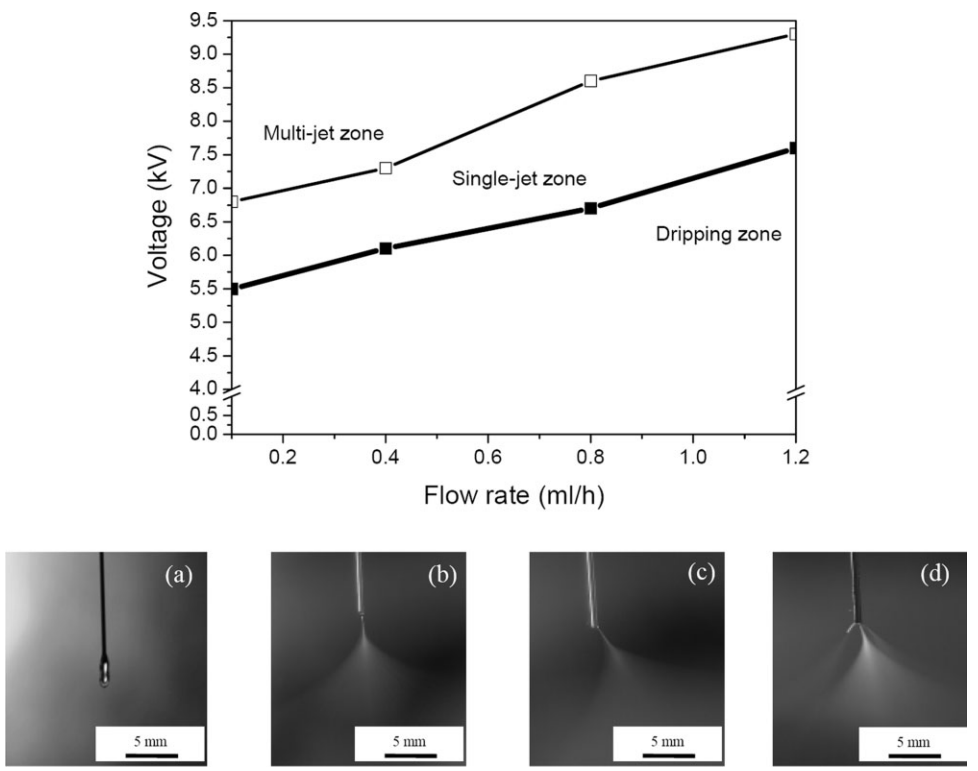

Figure 3 Spraying modes and critical voltages as functions of the flow rate. The electrospraying conditions were 7 wt % PS solutions in DMF and a ground-to-nozzle distance of 15 cm. The various modes [(a) dripping, (b) single jet near the critical voltage, (c) tilted single jet above the critical voltage, and (d) multijet] were distinguished by jetting observations.

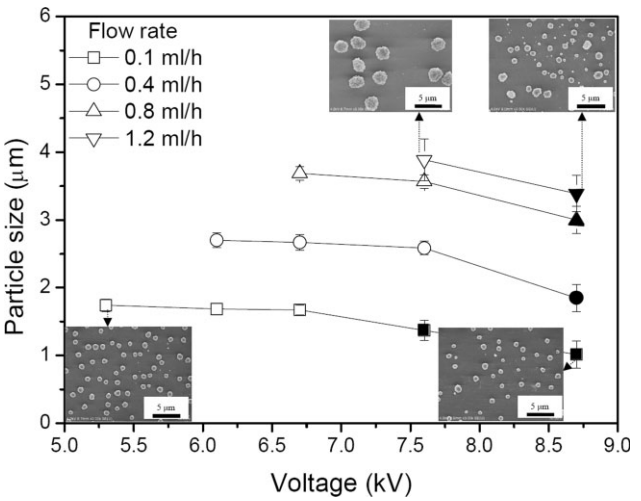

Figure 4 Particle size as a function of the flow rate and voltage. The inset SEM images show the solidified PS particles produced under the indicated conditions. Open and closed symbols correspond to the single-jet and multijet modes, respectively. The error bars are the standard deviations. The electrospraying concentration was 7 wt % in DMF.

the ground plate, THF and DMF solutions require at least 5- and 8-cm working distances, respectively. In this experiment, electrospraying was performed at a fixed working distance of 15 cm. This condition could have been dependent on other parameters that were fixed here, such as temperature.

The droplet size in the Ganan-Calvo equation [eq. (1)] is proportional to the flow rate (Q) on the order of $\sim Q^{1/2}$. We examined solidified PS particles as a function of both the flow rate and applied voltage, as shown in Figure 4. SEM images indicated a nearly spherical morphology for the solidified PS particles. The mean size of the PS particles increased with increasing flow rate at a fixed voltage, although the scaling exponent was smaller than predicted.[25–28] Voltage changes were followed by jet mode changes. In single-jet mode, the particles had similar sizes, regardless of the jet tilting angle. In multijet modes, it was still the case that the particle size scaled with liquid flow rate, but the size distribution of the particles was relatively larger than that for the single-jet mode. This indicated that the jet streams in the multijet mode might not have experienced uniform electrohydrodynamic forces. As a whole, a voltage in the single-jet window was necessary for a narrow particle size distribution, and a fine adjustment of flow rate was necessary to obtain proper particle size.

A series of mixed solvents was used to explore the effects of the solution properties on electrospraying, which directly influenced the development of a concentration gradient, skin formation, gelation, phase separation, and particle aggregation during consolidation of the droplets. Figure 5 presents the particle sizes and morphologies of solidified PS particles for two-solvent systems. For the cases of volume fractions of DMF of about 0.4 to 1.0, the PS particles had similar morphologies, despite changes in the surface tension, conductivity, and vapor pressure, as shown in Figure 2. When the DMF volume fraction was 0, PS solutions of 0.1 and 0.5 wt % resulted in particles with smooth surfaces. However, when the PS concentration was 1 wt % and the DMF volume fraction was 0.0 or 0.2, the PS particles had rough surfaces and large pores, which indicated the presence of phase-separation mechanisms (Fig. 5).

For the 0.0 volume fraction series, PS particles of 0.1 and 0.5 wt % had similar sizes, whereas the 1 wt % case generated particle sizes of about 5 μm. With 0.1 and 0.5 wt % PS solutions, a decrease in the DMF volume fraction did not significantly affect the particle size. However, for 1 wt % PS solutions, the particle size increased with increasing volume fraction of THF. Particle size did not reflect the linear change in conductivity of the solvents, as shown in Figure 2.

To further elucidate the morphological change that occurred during solvent evaporation, various pure solvents were used, as shown in Figure 6. For all of the solvent series, particle size increased with increasing concentration. An increase in boiling point generally correlated with a decrease in the particle size. For the cases of MC with the fastest evaporation rate among the systems, hollow particles were fabricated. In the SEM investigation of cleaved particles, the skin thickness was found to increase with increasing concentration. When the boiling point of

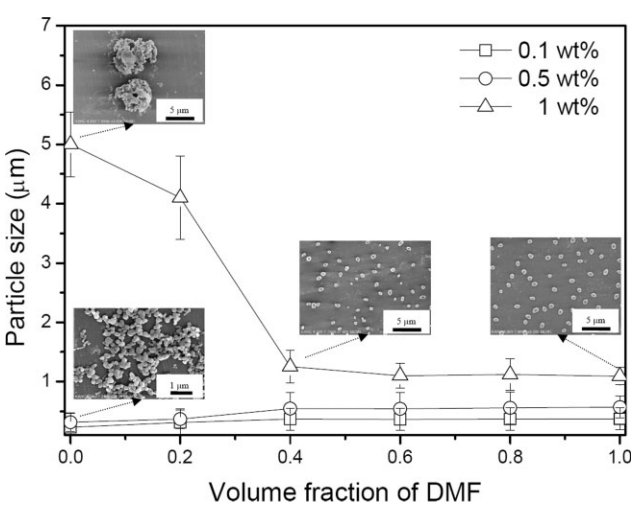

Figure 5 Particle size as a function of the volume fraction of DMF with various PS concentrations. The inset SEM images show the solidified PS particles produced under the indicated conditions. The error bars are the standard deviations. The electrospraying flow rate was 0.4 mL/h.

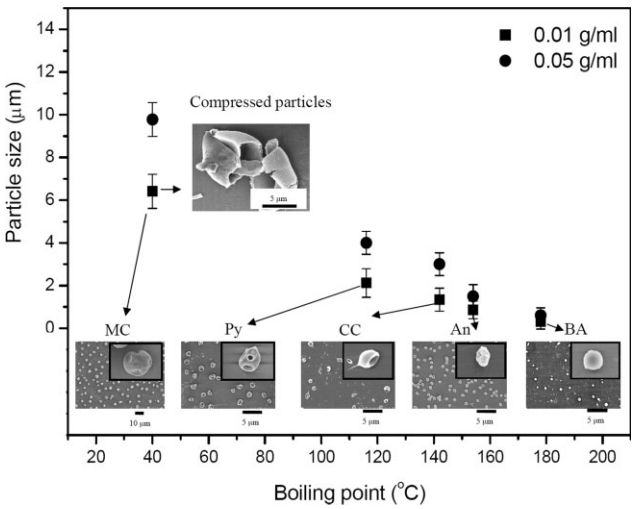

Figure 6 Particle size as a function of the boiling point of volatile solvents for 0.01 and 0.05 g/mL PS solutions. The SEM images exhibit solidified PS particles produced under the indicated conditions. In the case of MC, images of cleaved PS particle were examined after compression. The error bars are the standard deviations. The electrospraying conditions were an electrospraying flow rate of 0.4 mL/h and the critical voltage.

the solvents was high enough (>150°C), the particles had relatively spherical shapes and smooth surfaces (DMF and BA are good examples). The Py and CC solvents often resulted in cuplike morphologies, whereas the An cases showed porous structures similar to the THF-rich cases in Figure 5. The interesting morphologies of cuplike or hollow particles might have been generated by skin formation and subsequent contraction stress development. Our results prove that the evaporation process significantly affected the particle size and morphology.

DISCUSSION

The evaporation of solvent from charged droplets involves the complicated processes of heat/mass transfer and particle shrinkage. The size and morphology of particles fabricated with electrospraying are dependent on various variables, such as the type of solvent, surface charges, viscosity, humidity, temperature, Flory–Huggins interaction parameter between polymer and solvent, or molecular weight of the polymer. These parameters are often interrelated. Skin rheological properties at the surface might affect heat and mass transfer. However, the exact nature of the skin phase is a matter of controversy. The question of whether the skin phase is a region of viscoelastic fluid, a layer of soft gels, or a film of glassy polymer has not been answered clearly.[41] Regardless of the nature of the skin phase, the viscous fluid becomes elastic in the skin phase, and it is this elastic surface that dramatically decreases solvent diffusion and shrinkage. This phenomenon has been confirmed by experiments involving the solidification of polymer solutions deposited on a substrate and by several theoretical/physical models.[30,41–43]

In addition, the reduction of droplet size during solvent evaporation is closely related to the value of the Rayleigh limit. As shown in Figure 7, if the surface charge exceeded the Rayleigh limit, secondary breakup (Coulomb fission) could produce progeny droplets and charge/mass loss.[44,45] Also, secondary breakup resulted in a broader particle size distribution. After skin formation, the secondary breakup of droplets could hardly occur because of increased chain entanglement density and elasticity of the skin layer. Phase separation caused by poor solubility (high R_{ij} in Table I) could lead to porous structures, whereas homogeneous drying could also occur without any phase separation or significant skin formation. When the working distance was too short or the surface charge relaxed too quickly, the droplets underwent aggregation or film formation.

One of the most effective factors controlling consolidation may be the selection of the solvents. We studied two systems, a one-solvent system and a two-solvent (miscible) system. Similar to the case of Taylor cone formation, the drying process of actual droplets cannot be quantitatively predicted by theoretical treatments. The drying process of polymer solutions can be explained by a combination of diffusion, heat transfer, and thermodynamic energy equations, whereas contraction stress and actual non-Fickean diffusion are difficult to consider together.[26,43] For the polymer solutions in a single

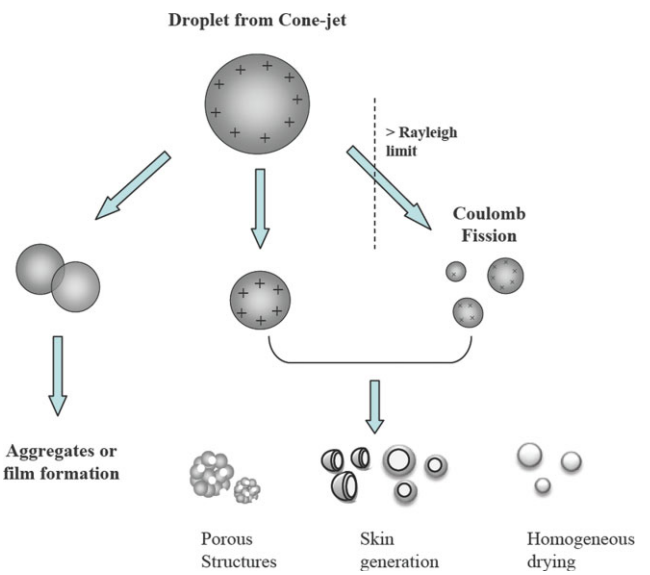

Figure 7 Schematic diagram of the particle formation mechanism of electrosprayed polymeric solutions. [Color figure can be viewed in the online issue, which is available at www.interscience.wiley.com.]

solvent, the drying rate initially stayed constant for a while and then rapidly decreased. As the surface diffusion barrier developed, the decrease leveled off. When two solvents were used, the initial rate was close to that for the more volatile solvent, and the final rate was close to that for the less volatile solvent. The overall change in drying rate was similar to that for a one-solvent system.

The previous drying rate observation tells us about the possible differences in concentrations and structures of the surface and center regions. The differences resulted in the formation of skin layers, which could account for the formation of inner holes and cuplike morphologies. However, porous surfaces more likely developed because of phase separation induced by solvent evaporation. Figure 7 shows the results of cases involving inhomogeneous drying.

Figures 5 and 6 show various solvent systems. The removal rate at the surface of a droplet could be faster than the internal mass transfer, and a skin layer could be generated before shrinkage occurred in the case of solvents whose boiling point was lower than 150°C. Polymer chains at the surface of a droplet were entangled during skin formation, and a solvent-rich phase developed in the center of the droplet. If the skin was strong enough to overcome the contraction pressure, hollow particles could be fabricated (e.g., MC cases). However, weak or defective skin layers (e.g., Py and CC cases) collapsed into cuplike particles to allow for dissipation of the contraction pressure.

The evaporation of a polymer solution can induce phase separation between polymer-rich and polymer-poor regions, which can reflect thermal fluctuation.[30] Phase separation might induce porous structures on the surface of droplets or hollow structures. As shown in Figure 5, PS particles had many pores after drying (1 wt % PS in THF).

In general, the solvent with the lower boiling point in two-solvent systems is always removed faster, and the other solvent is enriched in the solution.[46,47] For THF/DMF systems, the removal of THF was faster than the removal of DMF. During the drying of a droplet, three removal rate stages might be considered to understand the pore formation: (1) an initial stage involving the predominant removal of THF, (2) a middle stage of the removal of both THF and DMF, and (3) a final stage involving the predominant removal of DMF. The removal rate for the initial stage is almost constant, regardless of solvent composition.[47] Pore formation occurred for THF-rich cases with a high polymer concentration (Fig. 5). Therefore, phase separation and subsequent pore formation were likely triggered during the initial or middle removal rate stages.

Strictly speaking, all solidified particles will have a certain amount of radial inhomogeneity (e.g., skin), and the yielding of particles to contraction pressure affects particle morphology. These characteristics provide advantages and disadvantages in the use of the electrospraying technique for actual applications.

Among the parameters listed in Table I, boiling point seemed to be the parameter that showed the most systematic influence on the particle size, as shown in Figure 6. However, other parameters could always influence the mechanisms. The conductivity of each solvent was an important parameter that needs to be mentioned. According to previous research,[35,48,49] the diameter of a droplet is inversely proportional to the liquid conductivity to a certain power. The relaxation of surface charge can influence the droplet size and aggregation behavior. The temperature was fixed in our experiment, but it was an important parameter, too.

CONCLUSIONS

The effects of electrospraying parameters on the morphological and dimensional changes of solidified polymer particles were systematically investigated. Of the two particle-formation steps—liquid droplet formation and subsequent solidification—the solidification step distinctly influenced the final particle morphology, for which the choice of solvent was critical. The differences in concentration between the surface and center region of a droplet triggered the formation of skin layers, which could account for the formation of inner holes and cuplike morphologies. Porous structures on the particles seemed to result from phase separation induced by solvent evaporation. These inhomogeneous drying processes depended on various parameters, such as the evaporation rate and solvent viscosity. An increase in the rate of solvent evaporation generally increased particle size. However, this observation did not agree well with the scaling law of electrohydrodynamic jetting that has been developed for pure liquids. The results of this study provide a basis for the production of electrosprayed polymer particles for use in actual applications, such as drug delivery.

One of the authors (C.H.P.) thanks the Ministry of Knowledge Economy and Korea Industrial Technology Foundation through the Human Resource Training Project for Strategic Technology and Human Resource Development BK21 (Korea Research Foundation).

References

1. Englebienne, P.; Van Hoonacker, A. J Colloid Interface Sci 2005, 292, 445.
2. Narayan, K. S.; Manoj, A. G.; Nanda, J.; Sarma, D. D. Appl Phys Lett 1999, 74, 871.

3. Song, C. X.; Labhasetwar, V.; Murphy, H.; Qu, X.; Humphrey, W. R.; Shebuski, R. J.; Levy, R. J. J Controlled Release 1997, 43, 197.
4. Okubo, M. Adv Polym Sci 2005, 175, 1.
5. Manziek, L.; Langenmayr, E.; Lamola, A.; Gallagher, M.; Brese, N.; Annan, N. Chem Mater 1998, 10, 3101.
6. Kasai, H.; Nalwa, H. S.; Oikawa, H.; Okada, S.; Matsuda, H.; Minami, N.; Kakuta, A.; Ono, K.; Mukoh, A.; Nakanishi, H. Jpn J Appl Phys 1992, 31, L1132.
7. Mu, L.; Feng, S. S. J Controlled Release 2001, 76, 239.
8. Yeo, S.-D.; Kiran, E. J Supercrit Fluids 2005, 34, 287.
9. Ma, G. China Particuology 2003, 1, 105.
10. Hiroshi, Y.; Takeshi, H.; Kuniharu, I.; Masatsugu, S. Chaos 2005, 15, 047505.
11. Ude, S.; de la Mora, J. F.; Alexander, J. N.; Saucy, D. A. J Colloid Interface Sci 2006, 293, 384.
12. Fantini, D.; Zanetti, M.; Costa, L. Macromol Rapid Commun 2006, 27, 2038.
13. Gilbert, W. De Magnete; Dover: New York, 1958 (first published in Latin in 1600 and translated by P. F. Mottelay in 1893). This work was mentioned in Nat Phys 2008, 4, 149.
14. Zeleny, J. Phys Rev 1917, 10, 1.
15. Rayleigh, L. Philos Mag 1882, 14, 184.
16. Schweizer, J. W.; Hanson, D. N. J Colloid Interface Sci 1971, 35, 417.
17. Taflin, D. C.; Ward, T. L.; Davis, E. J. Langmuir 1989, 5, 376.
18. Alessandro, G.; Keqi, T. Phys Fluids 1994, 6, 404.
19. Taylor, G. Proc R Soc 1964, 280, 383.
20. Saville, D. A. Annu Rev Fluid Mech 1997, 29, 27.
21. Fenn, J. B.; Mann, M.; Meng, C. K.; Wong, S. F.; Whitehouse, C. M. Science 1989, 246, 64.
22. Borra, J. P.; Camelot, D.; Marijnissen, J. C. M.; Scarlett, B. J Electrostat 1997, 40, 633.
23. Jaworek, A. J Mater Sci 2007, 42, 266.
24. Jaworek, A. Powder Technol 2007, 176, 18.
25. Ogata, S.; Hatae, T.; Shoguchi, K.; Shinohara, H. Int Chem Eng 1978, 18, 488.
26. Yukio, T.; Yukio, I.; Toshio, Y. Bull JSME 1986, 29, 3737.
27. Fernandez De La Mora, J.; Loscertales, I. G. J Fluid Mech 1994, 260, 155.
28. Ganan-Calvo, A. M. J Aerosol Sci 1999, 30, 863.
29. Gupta, P.; Elkins, C.; Long, T. E.; Wilkes, G. L. Polymer 2005, 46, 4799.
30. Dayal, P.; Kyu, T. J Appl Phys 2006, 100, 043521.
31. Ding, L.; Lee, T.; Wang, C. H. J Controlled Release 2005, 102, 395.
32. Xie, J. W.; Wang, C. H. Biotechnol Bioeng 2007, 97, 1278.
33. Xu, Y. X.; Skotak, M.; Hanna, M. J Microencapsul 2006, 23, 69.
34. Liu, J.; Kumar, S. Polymer 2005, 46, 3211.
35. Loscertales, I. G.; Barrero, A.; Guerrero, I.; Cortijo, R.; Marquez, M.; Ganan-Calvo, A. M. Science 2002, 295, 1695.
36. Xie, J.; Lim, L. K.; Phua, Y.; Hua, J.; Wang, C.-H. J Colloid Interface Sci 2006, 302, 103.
37. Yeo, L. Y.; Gagnon, Z.; Chang, H.-C. Biomaterials 2005, 26, 6122.
38. Xie, J.; Ng, W. J.; Lee, L. Y.; Wang, C.-H. J Colloid Interface Sci 2008, 317, 469.
39. Smith, K. L.; Alexander, M. S.; Stark, J. P. W. J Appl Phys 2006, 99, 064909.
40. Fernandez de la Mora, J. Annu Rev Fluid Mech 2007, 39, 217.
41. Okuzono, T.; Ozawa, K.; Doi, M. Phys Rev Lett 2006, 97, 136103.
42. Pauchard, L.; Allain, C. Europhys Lett 2003, 62, 897.
43. Wong, S.-S.; Altinkaya, S. A.; Mallapragada, S. K. J Polym Sci Part B: Polym Phys 2005, 43, 3191.
44. Feng, X.; Bogan, M. J.; Agnes, G. R. Anal Chem 2001, 73, 4499.
45. Smith, J. N.; Flagan, R. C.; Beauchamp, J. L. J Phys Chem A 2002, 106, 9957.
46. Sacide Alsoy, J. L. D. AIChE J 1999, 45, 896.
47. Yoshida, M.; Miyashita, H. Chem Eng J 2002, 86, 193.
48. Ganan-Calvo, A. M.; Davila, J.; Barrero, A. J Aerosol Sci 1997, 28, 249.
49. Ganan-Calvo, A. M.; Lasheras, J. C.; Davila, J.; Barrero, A. J Aerosol Sci 1994, 25, 1121.
50. Brandrup, J.; Immergut, E. H. Polymer Handbook; Wiley-Interscience: New York, 1989.